

Organic-Free Synthesis of CHA-Type Zeolite Catalysts for the Methanol-to-Olefins Reaction

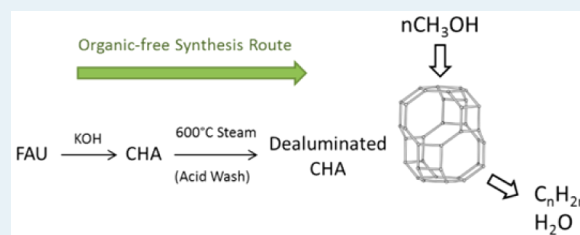
Yuewei Ji, Mark A. Deimund, Yashodhan Bhawe, and Mark E. Davis*

Chemical Engineering, California Institute of Technology, Pasadena, California 91125, United States

Supporting Information

ABSTRACT: Chabazite (CHA)-type zeolites are prepared from the hydrothermal conversion of faujasite (FAU)-type zeolites, dealuminated by high-temperature steam treatments (500–700 °C), and evaluated as catalysts for the methanol-to-olefins (MTO) reaction. The effects of temperature and partial pressure of water vapor during steaming are investigated. Powder X-ray diffraction (XRD) and Ar physisorption data show that the steam treatments cause partial structural collapse of the zeolite with the extent of degradation increasing with steaming temperature. ²⁷Al MAS NMR spectra of the steamed materials reveal the presence of tetrahedral, pentacoordinate, and octahedral aluminum. NH₃ and *i*-propylamine temperature-programmed desorption (TPD) demonstrate that steaming removes Brønsted acid sites, while simultaneously introducing larger pores into the CHA materials that make the remaining acid sites more accessible. Acid washing the steamed CHA-type zeolites removes a significant portion of the extra-framework aluminum, producing an increase in the bulk Si/Al ratio as well as the adsorption volume. The proton form of the as-synthesized CHA (Si/Al = 2.4) rapidly deactivates when tested for MTO at a reaction temperature of 400 °C and atmospheric pressure. CHA samples steamed at 600 °C performed the best among the samples tested, showing increased olefin selectivities as well as catalyst lifetime compared to the unsteamed CHA. Both lifetime and C₂–C₃ olefin selectivities are found to increase with increasing reaction temperature. At 450 °C, CHA steamed at 600 °C reached a combined C₂–C₃ olefin selectivity of 74.2% at 100% methanol conversion, with conversion remaining above 80% for more than 130 min of time-on-stream (TOS) before deactivating. More stable time-on-stream behavior is observed for 600 °C-steamed CHA that underwent acid washing: conversion above 90% for more than 200 min of TOS at 450 °C with a maximum total C₂–C₃ olefin selectivity of 71.4% at 100% conversion.

KEYWORDS: methanol-to-olefins, CHA, zeolite, organic-free, steaming



1. INTRODUCTION

The methanol-to-olefins (MTO) reaction is an industrially viable route for making the light olefins, ethylene and propylene, using feedstocks other than petroleum (e.g., natural gas, coal, and biomass).¹ The reaction can be carried out over solid acid catalysts such as microporous aluminosilicate² and silicoaluminophosphate (SAPO)^{3,4} molecular sieves. The industrial catalyst for the MTO reaction is SAPO-34,^{5,6} a small-pore SAPO molecular sieve with the chabazite (CHA) framework topology that is currently utilized in commercial MTO plants in China. Depending upon reaction conditions, SAPO-34 can convert methanol to ethylene and propylene at 85–90% selectivity.⁷ The high selectivity toward light olefins is attributed to the material's optimal acidity (acid site strength and density)⁸ as well as the topology of the CHA framework,^{9,10} consisting of relatively large cavities (8.35 Å × 8.35 Å × 8.23 Å¹¹) that are accessible through eight-membered ring (8MR) pore openings (3.8 × 3.8 Å¹¹). Only small linear molecules (alcohols and linear alkenes) can diffuse through the 8MR pores, while larger branched and aromatic compounds, including methylated aromatic intermediates,^{9,12} remain trapped inside the cages.

Despite its success, SAPO-34 suffers the shortcoming of requiring the use of an organic structure-directing agent (OSDA) to crystallize. Aluminosilicates (zeolites) also catalyze the reaction, but synthesizing them at high Si/Al ratios that are desirable for catalytic applications typically requires the use of OSDAs. The high cost and environmental concerns associated with removal of the OSDA from the materials prior to use has generated considerable interest in developing OSDA-free synthesis methods. Although the earliest synthetic zeolites were prepared in the absence of OSDAs, using only inorganic cations as the structure-directing species, they typically have high aluminum content (Si/Al < 5) and thus limited uses, particularly in applications requiring solid acidity.

CHA-type zeolites can be prepared in the absence of OSDAs, but their Si/Al ratios are too low to be of use in catalyzing reactions like MTO. However, it may be possible to remove aluminum from the framework through postsynthetic treatments, thereby modifying the acidity and catalytic behavior of the materials. Because CHA is an 8MR zeolite, the extracted

Received: February 24, 2015

Revised: May 1, 2015

Published: June 23, 2015

Table 1. Summary of steaming conditions, Si/Al ratios and acid site concentrations for dealuminated CHA samples

entry	sample	steaming conditions		Si/Al bulk	Si/Al _T ^b	acid site concentration by NH ₃ TPD [mmol/g]	acid site concentration by <i>i</i> -propylamine TPD [mmol/g]
		steaming temperature ^a	water saturator temperature				
1	CHA-S500B80	500 °C	80 °C	2.4	11	1.07	0.24
2	CHA-S600B80	600 °C	80 °C	2.4	16	0.94	0.30
3 ^c	CHA-S600B80A	600 °C	80 °C	7.8	12	0.80	0.39
4	CHA-S700B80	700 °C	80 °C	2.3	17	0.72	0.20
5	CHA-S600B90	600 °C	90 °C	2.5	16	0.84	0.29
6	CHA-S600B60	600 °C	60 °C	2.4	15	0.92	0.16
7	CHA-C600	600 °C	dry calcination	2.7	38	0.09	0.08

^aFurnace was held at temperature for 8 h for all samples. ^bCalculated from ²⁷Al NMR, Al_T denotes tetrahedral Al only ^cSteamed sample was acid washed with 0.1 N HCl for 2 h at 100 °C

aluminum cannot be removed from intact cages. However, if mesoporosity is formed during the dealumination, then it may be possible to extract the extra-framework aluminum via the larger pores. Here, we show that CHA-type zeolites synthesized without OSDAs can be subjected to dealumination to provide active MTO catalysts. This strategy may enable the preparation of low-cost MTO catalysts. Additionally, there are a number of other framework topologies that may be interesting catalysts for the MTO reaction that have yet to be evaluated because of their low Si/Al. The dealumination strategy provided here will allow for investigation of other framework types (we are currently exploring several other zeolites, and the results will be reported at a later time).

SSZ-13¹³ is the synthetic aluminosilicate analog of SAPO-34, and can be synthesized over a wide range of Si/Al ratios using the *N,N,N*-trimethyladamantylammonium OSDA. While also active for converting methanol to olefins, SSZ-13 deactivates more rapidly than SAPO-34, and initially produces a significant amount of C₁–C₄ alkanes.^{14,15} Recently, our research group showed that an SSZ-13 synthesized with high aluminum content (Si/Al = 5) could be steamed to obtain a catalyst with improved olefin selectivities and lifetime, comparable to that of an SSZ-13 with Si/Al = 15. Reaction data from this study are provided in the [Supporting Information](#) (Figures S1 and S2). In a similar study, Cartledge et al.¹⁶ prepared CHA-type zeolites at Si/Al ratios of greater than 2.5 using the hexamethylenetetramine OSDA, dealuminated the samples by steam and acid treatments, and observed improved olefin selectivities.

On the basis of these results, we hypothesized that a dealumination strategy could be applied to aluminum-rich CHA-type zeolites prepared without the use of an OSDA to create selective catalysts for converting methanol to light olefins. CHA-type zeolite is prepared from the hydrothermal conversion of zeolite Y (FAU) and then steamed at temperatures of 500, 600, or 700 °C to partially extract the framework aluminum. CHA steamed at 600 °C is additionally acid washed to remove the extra-framework aluminum. The effects of the dealumination treatments on the solids are analyzed by powder X-ray diffraction (XRD), energy-dispersive X-ray spectroscopy (EDS), and Ar physisorption. Removal of aluminum from the zeolite framework is observed by ²⁷Al and ²⁹Si MAS NMR. The acid site concentrations of the samples are measured by temperature-programmed desorption (TPD)

using NH₃ and *i*-propylamine. The catalytic performance of the materials is evaluated by the use of the MTO reaction.

2. EXPERIMENTAL SECTION

2.1. CHA Synthesis. CHA-type zeolites were prepared from the hydrothermal conversion of zeolite Y (FAU) following the method of Bourgogne et al.¹⁷ In a typical synthesis, 238 mL of deionized water was mixed with 32.2 mL of 45 wt % aqueous potassium hydroxide solution (Aldrich), to which 30 g of USY (Zeolyst, CBV712, SiO₂/Al₂O₃ = 12) was added. The mixture was shaken for about 30 s and heated in a sealed polypropylene vessel at 100 °C for 4 days under static conditions. The solid product was recovered by centrifugation, washed with water and acetone, and dried overnight at 100 °C. The as-synthesized product, which had potassium as the counterion (designated K-CHA), was ion-exchanged three times with 1 M aqueous ammonium nitrate solution at 90 °C for 2 h at a ratio of 100 mL of liquid per gram of solid to obtain the NH₄⁺ form (designated NH₄-CHA).

2.2. Steaming and Acid Washing Treatments. Table 1 provides a summary of the steaming and acid washing treatments. Steaming was conducted under atmospheric pressure in an MTI OTF-1200X horizontal tube furnace fitted with a 3 in. ID mullite tube. NH₄-CHA samples (approximately 1.2 g in a typical experiment) were loaded in ceramic calcination boats and placed in the center of the tube furnace. The furnace was ramped at 1 °C/min to the desired steaming temperature, held at temperature for 8 h, and then allowed to cool. The entire process was carried out under a flow of moist air that was created by bubbling zero-grade air at 50 cc/min through a heated water saturator (bubbler) upstream of the furnace. Samples were steamed at temperatures of 500, 600, and 700 °C with the bubbler held at 80 °C (water saturation pressure of 47.3 kPa) and the resulting materials designated CHA-S500B80, CHA-S600B80 and CHA-S700B80, respectively. The effect of the partial pressure of steam was investigated by two additional steaming experiments at 600 °C where the bubbler temperature was changed to 60 and 90 °C (water saturation pressures of 19.9 and 70.1 kPa, respectively). For each of the bubbler temperatures tested (60 °C, 80 and 90 °C), the air was approximately 50% saturated with water vapor. A dry calcination of NH₄-CHA was conducted in the same tube furnace for 8 h at 600 °C (1 °C/min ramp) under 50 cc/min of zero-grade air, and the

product was designated CHA-C600. A portion of the CHA steamed at 600 °C with the bubbler held at 80 °C was additionally acid washed with 0.1 N aqueous hydrochloric acid at a liquid-to-solid ratio of 100:1 (w/w) for 2 h at 100 °C in a sealed vessel. The product, designated CHA-S600B80A, was recovered by filtering, washed extensively with water, and dried overnight at 100 °C.

2.3. Characterization. Powder X-ray diffraction (XRD) patterns were obtained on a Rigaku MiniFlex II instrument with Cu K α radiation ($\lambda = 1.54184 \text{ \AA}$) at a sampling window of 0.01° and scan speed of 0.05°/min. Scanning electron microscopy/energy dispersive spectroscopy (SEM/EDS) was used to determine the morphology and bulk elemental composition of the materials and was conducted on a ZEISS 1550VP instrument equipped with an Oxford X-Max SDD energy dispersive X-ray spectrometer. Powder patterns were normalized to the highest intensity peak.

Solid-state ^{27}Al MAS NMR spectra were acquired on a Bruker AM 300 MHz spectrometer operated at 78.2 MHz using a 90° pulse length of 2 μs and a cycle delay time of 1 s. Samples were loaded in a 4 mm ZrO $_2$ rotor and spun at 12 kHz. Chemical shifts were referenced to 1 M aqueous aluminum nitrate solution. Solid-state ^{29}Si MAS NMR spectra were acquired on a Bruker Avance 200 MHz spectrometer operated at 39.78 MHz with ^1H decoupling. A 90° pulse length of 4 μs and a cycle delay time of 60 s was used for recording. Samples were loaded in a 7 mm ZrO $_2$ rotor and spun at 4 kHz, and chemical shifts were referenced to tetramethylsilane. Reported spectra are scaled to the same maximum intensity.

Argon physisorption was conducted on a Quantachrome Autosorb iQ instrument. Prior to adsorption measurements, samples were outgassed by heating (at a rate of 10 °C/min) the sample under vacuum for 1 h at 80 °C, 3 h at 120 °C and 10 h at 350 °C. Adsorption isotherms were collected using argon at 87.45 K using the constant dose (quasi-equilibrium) method. Micropore volumes were obtained from the adsorption branch of the isotherms using the t -plot method ($0.1 < P/P_0 < 0.3$). Pore size analyses were obtained from the adsorption branches using the nonlocal density functional theory (NLDFT) model provided by Quantachrome's data reduction software (based on model of Ar at 87 K on a zeolite with cylindrical pores).

NH $_3$ and *i*-propylamine TPD were performed on each ammonium-exchanged, steamed CHA sample to quantify the number and accessibility of the Brønsted acid sites present. NH $_3$ TPD is able to titrate essentially all acid sites both external to and within the 8MR pore system, while *i*-propylamine only accesses acid sites external to the 8MR pore system (and in areas of mesoporosity created by the steam treatment), as *i*-propylamine is too large to fit within the 8MR pores. When *i*-propylamine desorbs from a Brønsted acid site, it reacts with the site to form propylene and ammonia. The propylene desorption peak was integrated to determine the number of Brønsted acid sites accessible to *i*-propylamine.

The materials were pelletized, crushed, and sieved, with particles between 0.6 and 0.18 mm being retained and loaded between quartz wool beds in a continuous-flow quartz-tube reactor (part of an Altamira AMI-200 reactor). A thermocouple inserted directly into the bed monitored temperature, and a Dymaxion mass spectrometer monitored desorbing products.

Once loaded, samples were heated to 150 °C for 1 h at 10 °C/min and then to 600 °C for 1 h at 10 °C/min in flowing helium (50 sccm) to remove any adsorbed species. For NH $_3$ TPD, samples were then cooled to 160 °C, and NH $_3$ was dosed

onto each sample. After a 6 h purge in flowing argon (50 sccm) at 50 °C to remove any physisorbed NH $_3$, the sample was heated to 600 °C at a rate of 10 °C/min in 30 sccm argon, while the mass spectrometer monitored desorbing products, namely, $m/z = 17$ fragments corresponding to NH $_3$. The sample was held at 600 °C for 2 h to ensure all species had fully desorbed. For *i*-propylamine TPD, after the initial heating to 600 °C, samples were cooled to 50 °C, and *i*-propylamine was dosed onto each sample by means of a vapor saturator. The sample was then purged in a flow of helium (50 sccm) for 6 h before heating to 600 °C at 10 °C/min, with the mass spectrometer monitoring the main propylene and NH $_3$ signals ($m/z = 41$ and 17, respectively) formed by the decomposition reaction of the *i*-propylamine at Brønsted acid sites in the sample.

2.4. MTO Reaction Testing. Samples used for reaction testing were approximately 200 mg of pure zeolite that had been pelletized, crushed and sieved to obtain particles between 0.6 mm and 0.18 mm. A sample was supported between glass wool beds in a tubular, continuous flow reactor. Prior to reaction, all samples were calcined in situ under a flow of breathing-grade air, during which the temperature was ramped at 1 °C/min to 150 °C, held for 3 h, then ramped at 1 °C/min to 580 °C and held for 12 h. The reaction was conducted at 350, 400, or 450 °C with a feed of 10% methanol/inert at a WHSV of 1.3 h $^{-1}$. Reaction testing of unsteamed CHA was conducted on a sample in the H $^+$ form (H-CHA), which was obtained by calcining the NH $_4$ -CHA in situ. Regeneration of spent catalysts was conducted in situ by heating at 1 °C/min from the reaction temperature to 580 °C, holding for 6 h, and then cooling at 1 °C/min back to the reaction temperature, all under a flow of breathing-grade air. Conversions and selectivities are computed on a carbon mole basis, and reported selectivities are normalized by the total selectivity of the products observed.

3. RESULTS AND DISCUSSION

3.1. Sample Characterizations. **3.1.1. Effect of Steaming Temperature and Acid Washing.** The powder XRD patterns of the as-synthesized NH $_4$ -CHA and the CHA samples steamed at 500–700 °C under the same steam partial pressure are shown in Figure 1. The baseline signal increases relative to the peaks for the steamed samples, indicating the presence of amorphous material and a loss of crystallinity upon steaming. Increasing the steaming temperature, and thus the severity of steaming, results in increasingly greater structural degradation, with the 700 °C-steamed sample showing the greatest loss in crystallinity. Further, the XRD peaks are shifted to lower d -spacings for the steamed samples, which can be attributed to contractions of the unit cell due to extraction of framework aluminum. The bulk Si/Al ratios of the steamed samples (Table 1) are essentially the same as that of the starting CHA (Si/Al = 2.4), accommodating for minor deviations that are within measurement error. Acid washing the 600 °C-steamed CHA sample results in additional degradation and produces an increase in the bulk Si/Al ratio from 2.4 to 7.8.

Indications that aluminum is removed from the zeolite framework after the steam and acid treatments are provided by the ^{27}Al MAS NMR spectra that are shown in Figure 2. The spectra of both the as-synthesized K-CHA (Supporting Information Figure S3) and NH $_4^+$ -exchanged CHA show a single sharp resonance centered at approximately 55 ppm, corresponding to tetrahedral, framework aluminum. In addition

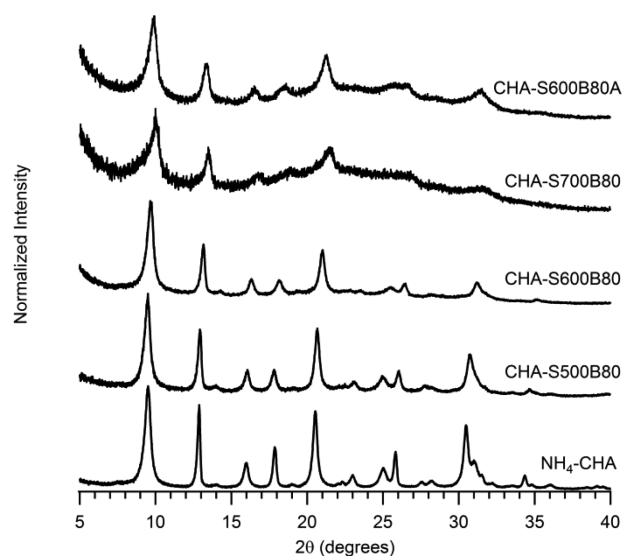


Figure 1. Powder XRD patterns of the as-synthesized CHA, CHA samples steamed at 500, 600, and 700 °C with water saturator at 80 °C, and the 600 °C-steamed and acid-washed CHA (bottom to top).

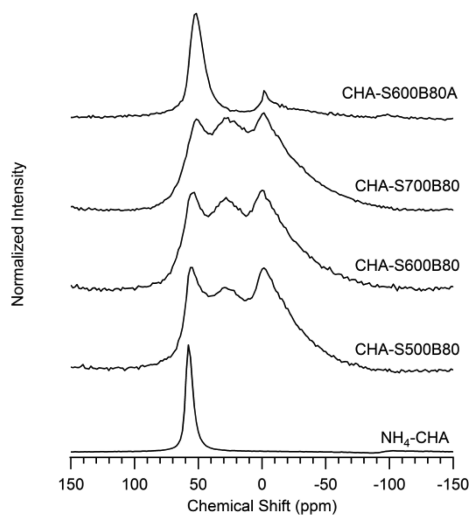


Figure 2. ^{27}Al MAS NMR spectra of the as-synthesized CHA, the CHA samples steamed at 500, 600, and 700 °C with water saturator at 80 °C, and the 600 °C-steamed and acid-washed CHA (bottom to top).

to this resonance, the spectra of the steamed samples show two additional resonances centered at approximately 30 and 0 ppm that are attributed to pentacoordinated and octahedral aluminum species, respectively. As the steaming temperature is raised from 500 to 700 °C, an increasing fraction of aluminum is converted from tetrahedral to penta- and hexacoordination (indicated by increases in the intensities of the resonances centered at 30 and 0 ppm relative to the resonance centered at 55 ppm). Accordingly, the silicon to tetrahedral aluminum (Si/Al_T) ratios (Table 1), calculated from the bulk Si/Al and deconvolution of the ^{27}Al NMR, increase with increasing steaming temperature. The intensities of the resonances associated with penta- and hexacoordinated aluminum are reduced after acid washing the 600 °C-steamed CHA, with nearly complete removal of the pentacoordinated aluminum species. These NMR data for the acid treated sample are consistent with the elemental analyses in that the bulk Si/Al

increases after acid treatment. These results also suggest that the bulk of the higher-coordinated (above 4) aluminum is extra-framework.

Further indication that the aluminum content of the zeolite framework changes after steaming is provided by the ^{29}Si MAS NMR spectra (Figure 3) of the steamed CHA. The spectrum of

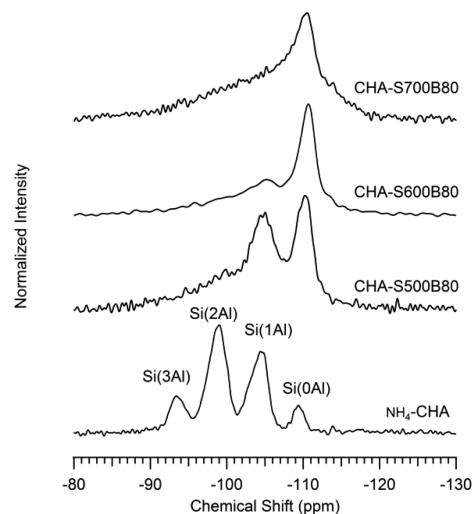


Figure 3. ^{29}Si MAS NMR spectra of the as-synthesized CHA, the CHA samples steamed at 500, 600, and 700 °C with water saturator at 80 °C, and the 600 °C-steamed and acid-washed CHA (bottom to top).

the as-synthesized $\text{NH}_4\text{-CHA}$ shows four resonances centered at approximately -109 ppm, -104 ppm, -98 ppm, -93 ppm, that can be attributed to Si(0Al), Si(1Al), Si(2Al) and Si(3Al) environments, respectively. The silicon environment changes to predominantly Si(0Al) and Si(1Al) after steaming, with the Si(0Al) resonance becoming the largest peak.

Figure 4A shows the full Ar physisorption isotherms of the as-synthesized $\text{NH}_4\text{-CHA}$ and steamed CHA samples along with the isotherm of a pure silicon dioxide sample (Si CHA) that is used as a control for illustrating the adsorption isotherm for a pure (cation-free) CHA material. The steamed CHA samples show decreased micropore adsorption volumes (Table 2) compared to the $\text{NH}_4\text{-CHA}$ due to partial collapse of the framework. The micropore filling region is illustrated in Figure 4B and shows the adsorption branches of the isotherms (on a semilogarithmic scale) normalized by the adsorption volume of Si CHA at $P/P_0 = 0.1$.

Acid washing the 600 °C-steamed CHA produces a significant increase in the adsorption volume that can be attributed to the removal of extra-framework aluminum localized within the channels and pores of the sample prior to acid leaching. This treatment, however, does not produce an increase in the micropore volume (Figure 4B).

At pressures above the micropore filling P/P_0 range, the adsorption isotherms of the steamed samples differ in shape from that of the $\text{NH}_4\text{-CHA}$ and Si CHA in that the adsorption volumes of the steamed samples increase continuously and at a higher rate per P/P_0 compared to the unsteamed samples. The NLDFT analyses of pore size distributions are illustrated in Figure 4C and show the cumulative pore volumes as a function of pore diameter. All of the samples show an initial steep increase in cumulative pore volume corresponding to micropore filling. Although the $\text{NH}_4\text{-CHA}$ does not show any

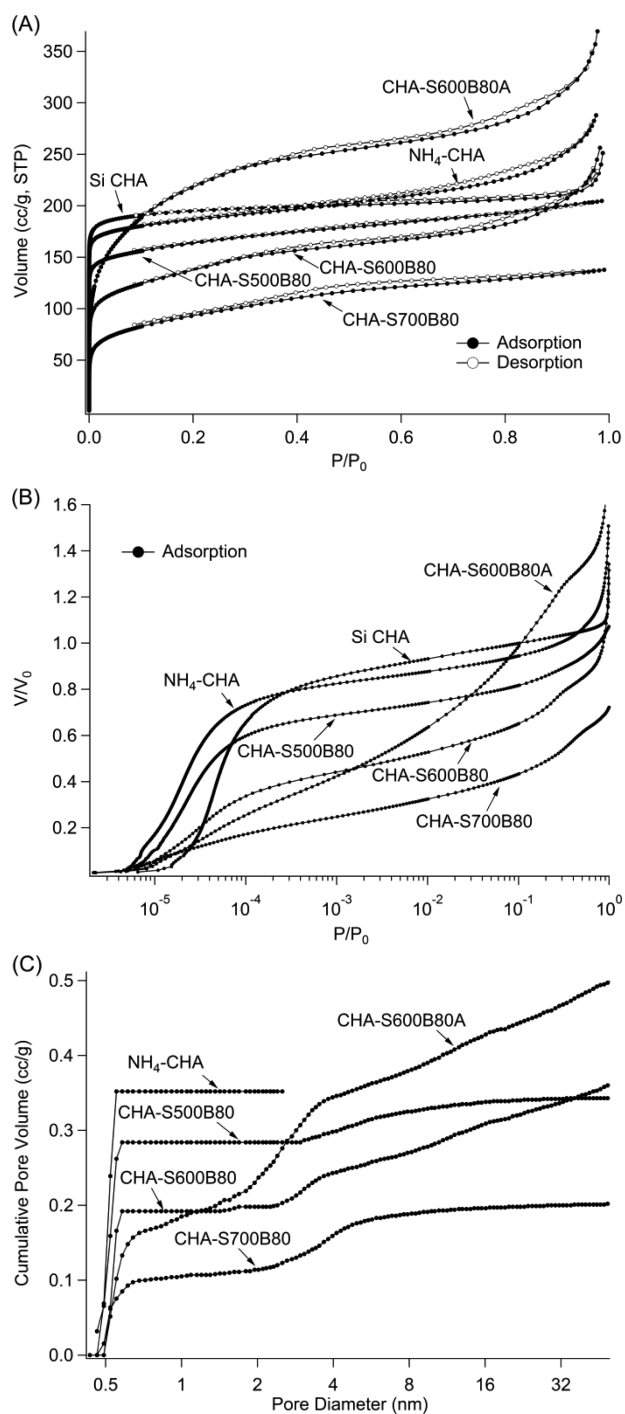


Figure 4. Ar physisorption isotherms of the as-synthesized and 500–700 °C-steamed CHA samples, and 600 °C-steamed and acid-washed CHA: (A) full isotherms, (B) normalized adsorption isotherms plotted on a semilogarithmic scale, and (C) NLDFT cumulative pore volume vs pore diameter.

additional pore filling in pores larger than approximately 0.5 nm in diameter, the steamed samples show a second step increase in cumulative pore volume for pores between 2 and 4 nm in diameter. These data suggest that mesopores are created by the steam treatments.

Entries 1, 2, and 4 of Table 1 also demonstrate how steaming decreases the total number of Brønsted acid sites from 3.75 mmol/g for the unsteamed material (NH_4 -CHA by NH_3 TPD) to 1.07, 0.94, and 0.72 mmol/g for the CHA samples

Table 2. Micropore Volumes of the As-Synthesized and Steamed CHA

sample	micropore volume (cc/g)
pure Si CHA	0.221
NH_4 -CHA	0.190
CHA-S500B80	0.149
CHA-S600B80	0.0765
CHA-S700B80	0.0379
CHA-S600B60	0.0466
CHA-S600B90	0.0753

steamed at 500, 600, and 700 °C, respectively. The number of Brønsted acid sites decreases as steaming temperature increases, consistent with increasing framework aluminum removal and degradation. These total acid site densities also correlate well with the predicted numbers based on the amount of tetrahedral aluminum remaining in each sample by ^{27}Al NMR.

The sites accessible by *i*-propylamine (presumably accessible via the mesopores introduced by steaming) exhibit a maximum with increasing steaming temperature at CHA-S600B80. This result suggests that the steaming process has an optimal temperature (600 °C for CHA) before framework degradation becomes too severe and access to acid sites decreases. For comparison, the unsteamed NH_4 -CHA has 0.08 mmol/g of acid sites by *i*-propylamine TPD. Acid washing of the steamed CHA-S600B80 sample (Entry 3 in Table 1) reveals the presence of fewer total Brønsted acid sites but a higher fractional accessibility, as indicated by the reduced NH_3 and increased *i*-propylamine acid site counts, respectively, from the TPDs.

These TPD results are consistent with the other characterization data for the samples that suggest steaming converts tetrahedral framework aluminum to pentacoordinate or octahedral aluminum species, consequently eliminating Brønsted acid sites (as seen via ^{27}Al NMR and NH_3 TPD), and introduces mesoporosity (as seen via Ar adsorption and *i*-propylamine TPD). The samples steamed at 600 °C demonstrate the best balance of access to Brønsted acid sites without excessive framework degradation.

3.1.2. Effect of Steam Partial Pressure. Figure 5 shows the XRD patterns of the samples steamed at 600 °C with varying partial pressures of steam. The XRD patterns show that lowering the steam partial pressure results in increased

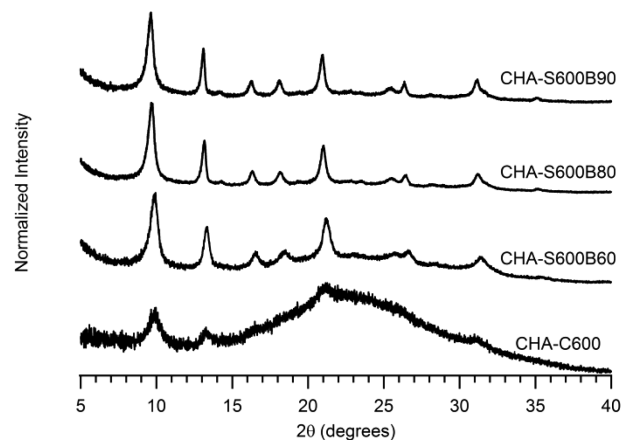


Figure 5. Powder XRD patterns of CHA samples steamed at 600 °C with varying partial pressures of steam.

amorphization, as indicated by an increasing baseline intensity relative to the peak intensities. Almost complete collapse of the structure is observed when $\text{NH}_4\text{-CHA}$ is calcined under dry air for 8 h at 600 °C.

The ^{27}Al MAS NMR spectra of the steamed samples (Figure 6), however, do not show significant differences in the relative

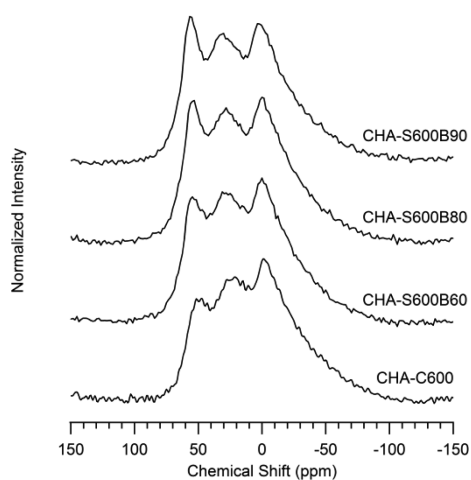


Figure 6. ^{27}Al MAS NMR spectra of CHA samples steamed at 600 °C with varying partial pressures of steam.

intensities of the tetrahedral, pentacoordinated, and hexacoordinated aluminum signals, although the intensity of the tetrahedral aluminum signal relative to the higher coordinated aluminum was the lowest for the CHA calcined under dry conditions. ^{29}Si NMR spectra of the samples steamed under varying steam partial pressures is shown in Figure 7, which shows differences in the silicon environments for the samples steamed under varying water vapor pressures.

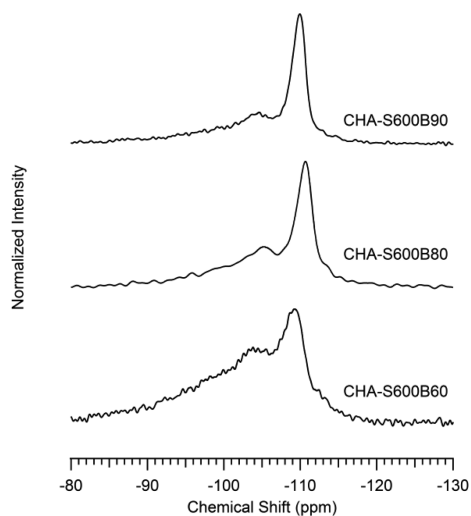


Figure 7. ^{29}Si MAS NMR spectra of CHA samples steamed at 600 °C in order of increasing steam partial pressures (bottom to top).

Ar physisorption measurements on the steamed samples (Figure 8A) show that with decreasing steam partial pressure, the samples show decreasing adsorption volume. This trend is also observed in the micropore filling region of the isotherms (Figure 8B) and corroborated by the intact micropore volumes (Table 2). Figure 8C indicates that the steamed samples have

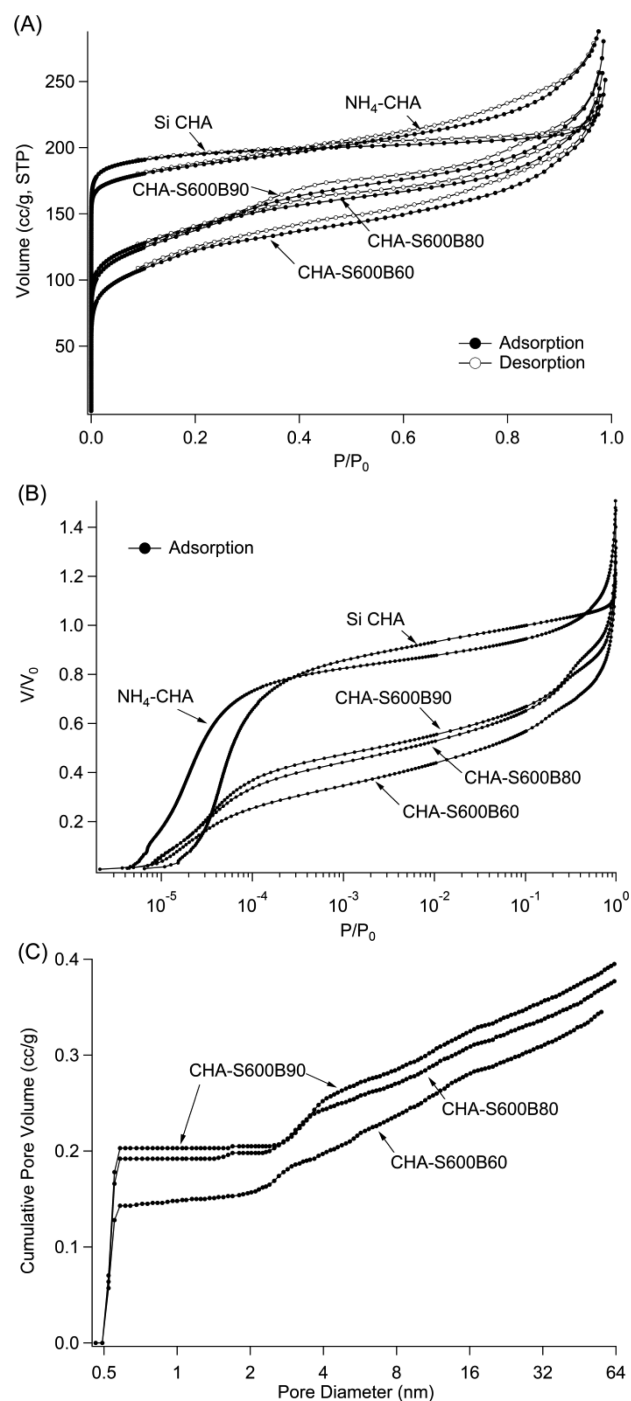


Figure 8. Ar physisorption isotherms of the as-synthesized and 600 °C-steamed CHA samples under varying steam partial pressures: (A) full isotherms, (B) normalized adsorption isotherms plotted on a semilogarithmic scale, and (C) NLDFT cumulative pore volume vs pore diameter.

essentially the same pore size distribution, showing a large step increase in cumulative pore volume for pores of 2 nm in diameter and larger.

Interestingly, as steam partial pressure decreases, the total Bronsted acid sites titrated by NH_3 TPD remain relatively similar (Entries 2, 5, and 6 in Table 1, consistent with the ^{27}Al NMR results), with a maximum value at CHA-S600B80. The *i*-propylamine TPD results are quite different, however, with the greatest accessibility observed for the two samples that were

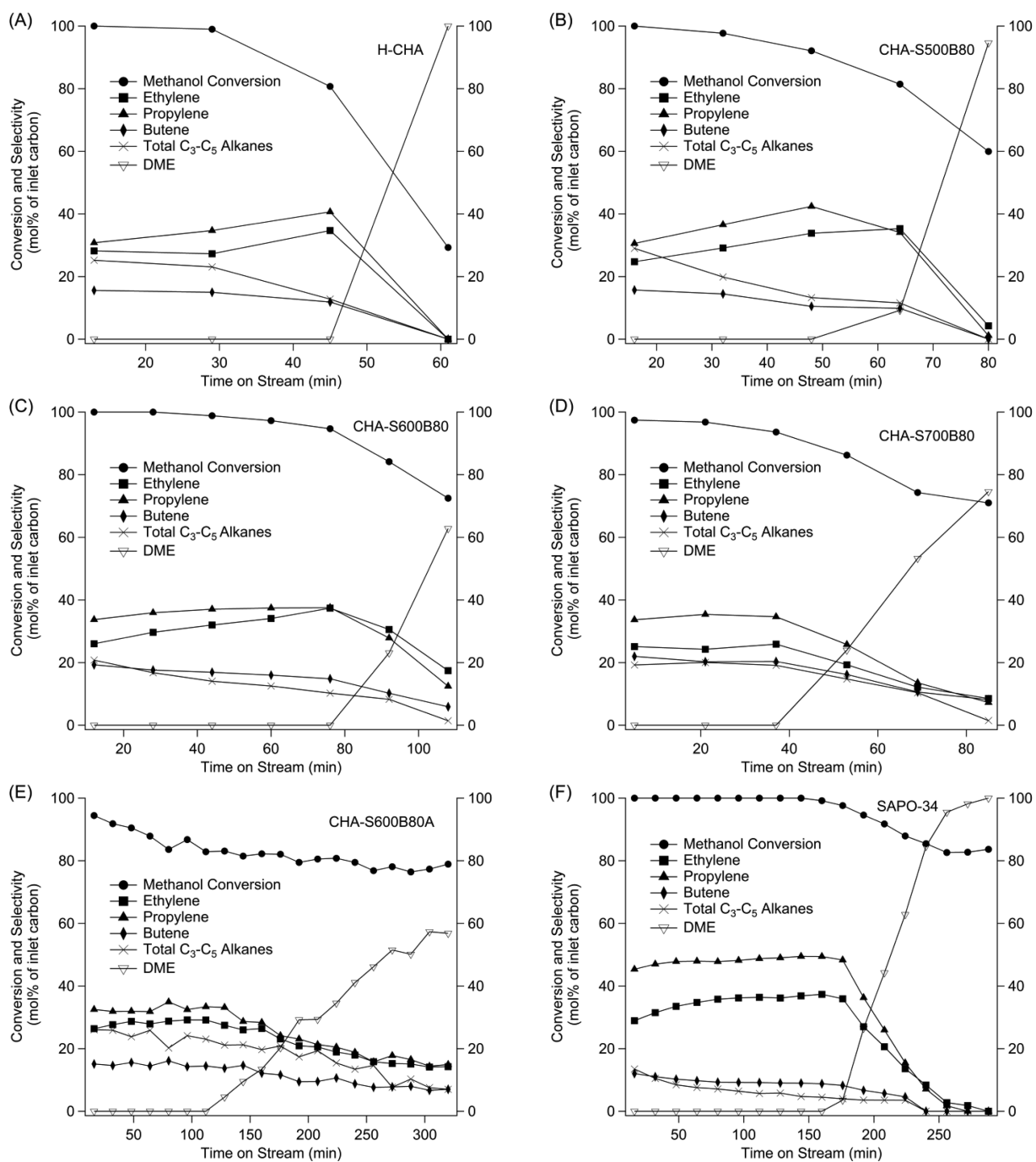


Figure 9. Representative MTO reaction data obtained at 400 °C for: (A) unsteamed H-CHA, (B) 500 °C-steamed CHA, (C) 600 °C-steamed CHA, (D) 700 °C-steamed CHA, (E) 600 °C-steamed and acid-washed CHA, and (F) SAPO-34.

steamed with the water saturator at 80 and 90 °C (CHA-S600B80 and CHA-S600B90, respectively). The sample with the lowest steam partial pressure, CHA-S600B60, has approximately half the *i*-propylamine accessibility of these other samples.

The trend of increased degradation with decreasing steam partial pressure is opposite of what has been reported for larger pore zeolites such as zeolite Y (FAU)^{18,19} and ZSM-5 (MFI).²⁰ Our steaming experiments with zeolite Y at 550 and 650 °C using a similar steam procedure to those reported by Wang et al.,¹⁹ are consistent with the literature results in that zeolite Y samples calcined in the presence of steam undergo greater dealumination compared to samples calcined in dry air.

Characterizations (powder XRD patterns and ²⁷Al NMR) for the 550 and 650 °C-steamed zeolite Y samples are provided in the [Supporting Information](#) (Table S1 and Figures S4–S7). However, when zeolite Y is steamed under more severe conditions (8 h at 800 °C) using the same steaming procedure that was used with the CHA zeolites, the results ([Supporting Information](#) Table S1 and Figures S8–S9) show the reversed trend of greater degradation with decreasing steam partial pressure, consistent with the behavior of the CHA zeolites. Furthermore, steam treatment of CHA at milder conditions (3 h at 500 °C) using the 550 and 650 °C Y steaming procedure produces increasing dealumination with increasing steam partial pressure ([Supporting Information](#) Table S1 and Figures S10–

Table 3. Maximum Combined C₂–C₃ Olefin Selectivities near Complete Conversion, and Deactivation Times of Catalysts Tested

sample	reaction temperature	maximum methanol conversion	combined C ₂ –C ₃ olefin selectivity at maximum methanol conversion	time to deactivation (g-MeOH/g-cat) ^a
H-CHA	400 °C	100.0%	59.0%	1.3
CHA-S500B80	400 °C	100.0%	55.3%	1.6
CHA-S600B80	350 °C	98.6%	58.6%	1.2
	400 °C	100.0%	65.6%	2.3
	450 °C	100.0%	74.2%	3.2
CHA-S700B80	400 °C	97.4%	58.8%	1.4
CHA-S600B80A	400 °C	94.4%	58.9%	5.0
	450 °C	100.0%	71.4%	>9.0
SAPO-34	400 °C	100.0%	86.3%	>9.8

^aFirst time point where methanol conversion drops below 80%

S11), consistent with the behavior of zeolite Y at the lower steaming temperatures. The similar behaviors between CHA and zeolite Y at these steaming conditions suggest that the trend reported here is not unique to CHA.

It has been proposed that the steaming involves hydrolyses of Al–O–Si bonds by water vapor at high temperatures, resulting in extra-framework aluminum species and the formation of vacant silanol nests.^{19,21,22} As an increasing number of the framework aluminum is extracted, portions of the zeolite collapse, forming amorphous regions. Investigations on the steam dealumination of Y zeolites further suggest that in the presence of steam, silicon may migrate in the form of orthosilicic acid (H₄SiO₄) to fill in the aluminum vacancies and thus “heal” the structure so that the resulting structure shows increased thermal stability.^{22,23}

It is likely that a similar stabilization process may be occurring during the heating period for the zeolites studied here. When heated to temperatures at which the zeolite normally becomes amorphous under dry conditions (600 °C for CHA and 800 °C for Y in this study), the presence of steam provides stabilization of the structure. Due to the slow ramp rate (1 °C/min) used during the steaming experiments for CHA and Y where the reversed trend of increased degradation with decreasing steam partial pressure was observed, the samples spend approximately the first half of the duration of the steaming experiment in heating under a steam atmosphere. A significant portion of the steaming process would thus occur in the heating period, during which the dealumination and healing steps described above are occurring at the same time. Under the higher steam partial pressures tested, healing of the framework may be facilitated and occurs at a rate that is fast enough to compensate for the dealumination process; thus, the structure is stabilized during the heating period. At a low steam partial pressure, the rate of healing could be too slow to compensate for dealumination and dehydroxylation, and thus, significant loss of crystallinity occurs. The ²⁹Si NMR of the samples steamed under varying steam partial pressures suggest that as the steam partial pressure is increased, the Si(OAl) peak grows in intensity relative to the downfield peaks, which would be consistent with increasing formation of Si–O–Si bonds with increasing availability of water during steaming.

3.2. MTO Reaction Testing. **3.2.1. Effect of Steaming Temperature and Acid Washing.** Figure 9 illustrates representative TOS reaction data obtained at 400 °C for the as-synthesized CHA, the CHA samples steamed at 500–700 °C with the water saturator at 80 °C, and a SAPO-34. Each of the catalysts is initially active in producing C₂–C₄ olefins when

methanol conversion is close to 100%. With increasing TOS, methanol conversion decreases, and is accompanied by a decrease in olefin selectivities and a simultaneous increase in dimethyl ether (DME) production. C₃–C₅ alkanes, mainly propane and butane, are also observed among the products at the start of the reaction, with selectivities decreasing with increasing TOS. Lower alkanes (methane and ethane) are not observed among the products.

Table 3 provides a summary of the reaction data that includes the maximum methanol conversion, maximum combined C₂–C₃ olefin selectivity at maximum conversion and the approximate time to deactivation (arbitrarily defined as the first time point where the conversion drops below 80%). The as-synthesized CHA, while initially active in producing ethylene and propylene, has the shortest catalyst lifetime. Methanol conversion starts at 100%, but decreases rapidly after approximately 45 min (0.93 g-MeOH/g-cat) TOS, and DME becomes the main reaction product. The fast deactivation may be attributed to the high framework aluminum content of the as-synthesized CHA (Si/Al = 2.4) that leads to rapid coke deposition.

Whereas deactivation occurs abruptly for the as-synthesized CHA, the steamed materials show more gradual deactivation profiles that vary depending on the severity of steaming. CHA steamed at 500 °C has a slightly improved lifetime compared to the as-synthesized CHA. Methanol is initially completely converted and remains above 80% conversion for 64 min (1.3 g-MeOH/g-cat) TOS. However, olefin selectivities for CHA-S500B80 are comparable to the unsteamed CHA.

CHA steamed at 600 °C shows the most stable reaction profile and longest lifetime among the steamed samples. Methanol conversion starts at 100% and remains above 80% for more than 92 min (2.0 g-MeOH/g-cat) TOS before deactivation occurs, with DME becoming the main product. Importantly, improved olefin selectivities are also observed for this sample. C₂–C₃ olefin selectivities increase gradually with increasing TOS when conversion is near 100% and reach maximum selectivities of 29.7% and 35.9%, respectively, at complete conversion, and approaches olefin selectivities for SAPO-34 (Figure 9F). Upon regeneration of the spent catalyst, similar olefin selectivities are observed with only a slight decrease in catalyst lifetime (Supporting Information Figures S12 and S13).

The lifetime of the 600 °C-steamed CHA is improved further after acid washing (Figure 9E). Methanol conversion decreases slowly and remains steady around 80% until approximately 240 min (5.0 g-MeOH/g-cat) TOS. The combined ethylene and

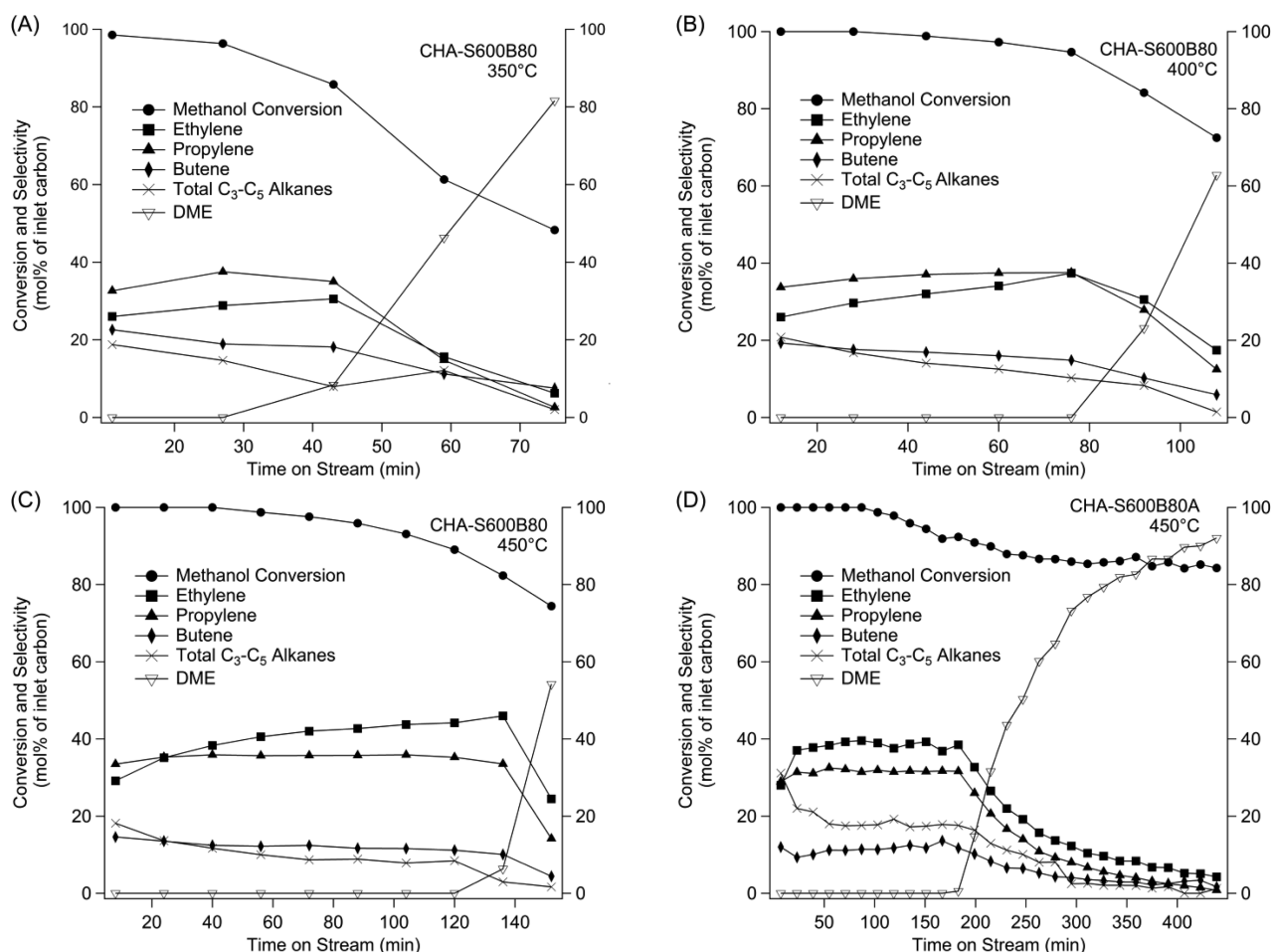


Figure 10. Representative MTO reaction data for 600 °C-steamed CHA (CHA-S600B80) obtained at reaction temperatures of (A) 350 °C, (B) 400 °C, (C) 450 °C and (D) 600 °C-steamed and acid-washed CHA (CHA-S600B80A) at a reaction temperature of 450 °C.

propylene selectivity remains steady at approximately 61% for 100 min TOS before gradually declining.

Increasing the steaming temperature further to 700 °C gives poorer MTO activity compared to CHA-S600B80, likely due to the increased severity of steaming at 700 °C. Ethylene and propylene reach selectivities of 24.3% and 35.4%, respectively, at 96.8% methanol conversion (21 min TOS). Conversion drops below 80% by approximately 60 min TOS, giving a reaction profile similar to the 500 °C-steamed CHA.

The improvements in selectivities and catalyst lifetime of the 600 °C-steamed CHA may be attributed to modifications in the acidity of the catalysts resulting from the extraction of framework aluminum. It is also likely that the mesoporosity created by steaming plays a role in the extended lifetimes. It has been observed that the introduction of mesopores in microporous zeolite catalysts facilitates mass transport to the micropores and leads to longer catalyst lifetimes.²⁴ This trend has been reported by Wu et al.,²⁵ who evaluated hierarchical SSZ-13 that was synthesized using the *N,N,N*-trimethyladamantylammonium OSDA in combination with a mesoporegen. These introduced mesopores result in improved lifetimes for the MTO reaction by allowing greater utilization of the micropore volume. As demonstrated by the NH₃ and *i*-propylamine TPD data, the 600 °C-steamed CHA sample appears to have the best balance of intact Brønsted acid sites and access to those sites via the mesoporosity introduced by the

steaming process that could account for the excellent reaction behavior observed.

3.2.2. Effect of Reaction Temperature. The effects of reaction temperature on the activity of CHA-S600B80 and CHA-S600B80A are illustrated in Figure 10. The most apparent trend in the reaction profiles for CHA-S600B80 when the reaction temperature is increased from 350 to 450 °C is the increase in catalyst lifetime. At 350 °C, methanol conversion is initially near 100% but declines below 80% after approximately 59 min (1.3 g-MeOH/g-cat) of TOS, while at 400 °C, the lifetime was 108 min (2.3 g-MeOH/g-cat). Increasing the reaction temperature further to 450 °C results in the longest lifetime at 152 min (3.2 g-MeOH/g-cat). Further, the maximum combined ethylene and propylene selectivity increases at 450 °C to 74.2% at 100% conversion, approaching olefin selectivities observed for SAPO-34 (Figure 9F).

Similarly, the acid-washed sample shows increases in lifetime and olefin selectivities at 450 °C. CHA-S600B80A converts methanol to ethylene and propylene steadily at an average of 69% combined selectivity for almost 200 min (4.1 g-MeOH/g-cat) TOS before DME becomes the main product. Further, ethylene selectivities increase for both CHA-S600B80 and CHA-S600B80A when the reaction temperature is increased from 400 to 450 °C so that more ethylene than propylene is produced at 450 °C. Regeneration of CHA-S600B80A at 450 °C results in some loss in olefin selectivities and lifetime (Supporting Information Figures S14 and S15).

CONCLUSION

CHA-type zeolites were prepared from the hydrothermal conversion of zeolite Y, NH_4^+ -exchanged, and dealuminated postsynthetically by steam and acid treatments to create selective catalysts for converting methanol to olefins. Characterizations by XRD and Ar physisorption of the steamed samples showed that partial collapse of the framework occurs during the steaming process with the degree of degradation increasing with steaming temperature. ^{27}Al MAS NMR spectra of the steamed samples revealed the presence of tetrahedral, pentacoordinate, and octahedral aluminum species. NH_3 and *i*-propylamine TPD results further corroborated that steaming converted tetrahedral aluminum to pentacoordinate and octahedral species while also introducing pores larger than 8MR pores to the samples (simultaneously reduced the number of total Brønsted acid sites, but made them more accessible). As steaming temperature increases, the total Brønsted acid sites decreased, but accessibility via mesopores exhibited a maximum when samples were steamed at 600 °C.

When evaluated for the MTO reaction, the unsteamed H-CHA (Si/Al = 2.4) deactivated quickly, whereas the steamed samples showed longer lifetimes and increased olefin selectivities. CHA steamed at 600 °C achieved the highest olefin selectivities (comparable to that of the commercial catalyst) and lifetime among the steamed samples, and the activity was retained upon regeneration of the spent catalyst. The results presented here show that the acidity and catalytic behavior of an aluminum-rich CHA zeolite prepared without using an OSDA can be modified by postsynthetic dealumination treatments to create a selective catalyst for converting methanol to olefins. It is likely that this dealumination strategy may be effective for preparing useful catalysts starting from small-pore zeolites of other topologies that are currently of interest for applications such as MTO and deNO_x.

ASSOCIATED CONTENT

Supporting Information

The Supporting Information is available free of charge on the ACS Publications website at DOI: 10.1021/acscatal.5b00404.

Reaction data for the steaming study with SSZ-13, further characterization of the synthesized materials, reaction data for regenerated CHA samples, and characterization of steamed Y samples are provided in additional tables and figures (PDF)

AUTHOR INFORMATION

Corresponding Author

*E-mail: mdavis@chem.caltech.edu.

Notes

The authors declare no competing financial interest.

ACKNOWLEDGMENTS

The authors thank the Dow Chemical Company for financial support of this work. The authors also thank Drs. Andrzej Malek, Jonathan Lunn, and Yu Liu from the Dow Chemical Company for helpful discussions.

REFERENCES

(1) Vora, B.; Chen, J. Q.; Bozzano, A.; Glover, B.; Barger, P. *Catal. Today* **2009**, *141*, 77–83.

(2) Froment, G. F.; Dehertog, W. J. H.; Marchi, A. J. In *Catalysis*; Spivey, J. J., Ed; Specialist Periodical Reports: Catalysis, Vol. 9; The Royal Society of Chemistry: Cambridge, 1992; p 1–64.

(3) Dai, W.; Wang, X.; Wu, G.; Guan, N.; Hunger, M.; Li, L. *ACS Catal.* **2011**, *1*, 292–299.

(4) Kaiser, S. W. Using silicoaluminophosphate molecular sieve catalyst. U.S. Patent 4,499,327, February 12, 1985.

(5) Liang, J.; Li, H.; Zhao, S.; Guo, W.; Wang, R.; Ying, M. *Appl. Catal.* **1990**, *64*, 31–40.

(6) Vora, B. V.; Marker, T. L.; Barger, P. T.; Nilsen, H. R.; Kvisle, S.; Fuglerud, T. In *Studies in Surface Science and Catalysis*; de Pontes, M., Espinoza, R. L., Nicolaidis, C. P., Scholtz, J. H., Scurrill, M. S., Eds.; Elsevier: Amsterdam, 1997; Vol. 107, pp 87–98.

(7) Chen, J. Q.; Bozzano, A.; Glover, B.; Fuglerud, T.; Kvisle, S. *Catal. Today* **2005**, *106*, 103–107.

(8) Bleken, F.; Bjørgen, M.; Palumbo, L.; Bordiga, S.; Svelle, S.; Lillerud, K.-P.; Olsbye, U. *Top. Catal.* **2009**, *52*, 218–228.

(9) Haw, J. F.; Marcus, D. M. *Top. Catal.* **2005**, *34*, 41–48.

(10) Wilson, S.; Barger, P. *Microporous Mesoporous Mater.* **1999**, *29*, 117–126.

(11) Baerlocher, C.; McCusker, L. B.; Olson, D. H. *Atlas of Zeolite Framework Types*, 6th revised ed.; Elsevier: Amsterdam, 2007.

(12) Arstad, B.; Nicholas, J. B.; Haw, J. F. *J. Am. Chem. Soc.* **2004**, *126*, 2991–3001.

(13) Zones, S. I. Zeolite SSZ-13 and its method of preparation. U.S. Patent 4,544,538, October 1, 1985.

(14) Yuen, L.-T.; Zones, S. I.; Harris, T. V.; Gallegos, E. J.; Auroux, A. *Microporous Mater.* **1994**, *2*, 105–117.

(15) Zhu, Q. J.; Kondo, J. N.; Ohnuma, R.; Kubota, Y.; Yamaguchi, M.; Tatsumi, T. *Microporous Mesoporous Mater.* **2008**, *112*, 153–161.

(16) Cartledge, S.; Patel, R. In *Studies in Surface Science and Catalysis*; Jacobs, P. A., vanSanten, R. A., Eds.; Elsevier: Amsterdam, 1989; Vol. 49, pp 1151–1161.

(17) Bourgogne, M.; Guth, J. L.; Wey, R. Process for the preparation of synthetic zeolites, and zeolites obtained by said process. U.S. Patent 4,503,024, March 5, 1985.

(18) Engelhardt, G.; Lohse, U.; Patzelová, V.; Mägi, M.; Lippmaa, E. *Zeolites* **1983**, *3*, 233–238.

(19) Wang, Q. L.; Giannetto, G.; Torrealba, M.; Perot, G.; Kappenstein, C.; Guisnet, M. *J. Catal.* **1991**, *130*, 459–470.

(20) Lago, R. M.; Haag, W. O.; Mikovsky, R. J.; Olson, D. H.; Hellring, S. D.; Schmitt, K. D.; Kerr, G. T.; In *Studies in Surface Science and Catalysis*; Murakami, Y., Iijima, A., Ward, J. W., Eds.; Elsevier: Amsterdam, 1986; Vol. 28, pp 677–684.

(21) Malola, S.; Svelle, S.; Bleken, F. L.; Swang, O. *Angew. Chem., Int. Ed.* **2012**, *51*, 652–655.

(22) Lutz, W. *Adv. Mater. Sci. Eng.* [Online] **2014**, *2014*, DOI:10.1155/2014/724248.

(23) Scherzer, J. In *Catalytic Materials: Relationship Between Structure and Reactivity*. Whyte, T. E.; Dalla Betta, R. A.; Derouane, E. G.; Baker, R. T. K., Eds.; ACS Symposium Series 248; American Chemical Society: Washington, DC, 1984; pp 157–200.

(24) Hartmann, M. *Angew. Chem., Int. Ed.* **2004**, *43*, 5880–5882.

(25) Wu, L.; Degirmenci, V.; Magusin, P. C. M. M.; Lousberg, N. J. H. G. M.; Hensen, E. J. M. *J. Catal.* **2013**, *298*, 27–40.